

Ballistic electrons in an open square geometry: Selective probing of resonant-energy states

I. V. Zozoulenko

Department of Physics and Measurement Technology, Linköping University, S-581 83 Linköping, Sweden

R. Schuster

*Braun Center for Submicron Research, Weizmann Institute of Science, Rehovot 76100, Israel
and Sektion Physik, LMU München, Geschwister-Scholl-Platz 1, 80539 München, Germany*

K. -F. Berggren

Department of Physics and Measurement Technology, Linköping University, S-581 83 Linköping, Sweden

K. Ensslin

*Festkörperphysik, ETH Zürich and PSI, 8093 Zürich, Switzerland
and Sektion Physik, LMU München, Geschwister-Scholl-Platz 1, 80539 München, Germany*

(Received 28 October 1996)

We report on the interplay between classical trajectories and quantum-mechanical effects in a square geometry. At low magnetic fields the four-terminal resistance is dominated by phenomena that depend on ballistic trajectories in a classical billiard. Superimposed on these classical effects are quantum interference effects manifested by highly periodic conductance oscillations. Numerical analysis shows that these oscillations are directly related to excitations of particular eigenstates in the square. In spite of open leads, transport through an open cavity is effectively mediated by just a few (or even a single) resonant-energy states. The leads injecting electrons into the cavity play a decisive role in a selection of the particular set of states excited in the dot. The above selection rule sets a specific frequency of the oscillations seen in the experiment.

[S0163-1829(97)50316-X]

Ballistic semiconductor quantum dots are rewarding objects for studying relations between quantum mechanics and corresponding semiclassical electron dynamics. A number of semiclassical predictions have been recently made for transport characteristics of ballistic quantum dots whose classical counterparts are chaotic or regular, respectively.¹ Many of the above predictions have been tested in recent experiments² and the difference in transport properties of chaotic and regular billiards has been found.³

Transport characteristics of open dots are often analyzed on the basis of the known properties of the corresponding closed structure.^{4,5} Recent theoretical studies of the effects of leads on the electron dynamics in open dots are rather contradictory. Reference 6 shows that the statistics of the spectra for open dots are exactly the same as that of the corresponding closed systems. At the same time, the results⁷⁻⁹ suggest that the leads attached to the dot may change the level statistics, so that a transition to chaos can occur in a nominally regular system. Besides, when dot openings become large enough, the eigenenergy levels interact and acquire a finite broadening due to the finite lifetime of electrons in the dot. This energy broadening might be much bigger than the mean energy level separation, resulting in overlapping of many resonances. Under these conditions it is not clear whether a discussion of transport through the dot based on the properties of the Hamiltonian of the closed structure is still meaningful for the open system.

In this paper we investigate ballistic transport in an open, nominally regular square geometry. We show that despite the lifetime broadening induced by the leads, transport through the structure is still effectively mediated by just a few (or even a single) regular eigenstates of the isolated square. The

geometry of the leads injecting electrons into the cavity plays a decisive role in the selection of the particular eigenstates excited in the dot. The above selection rule sets a specific frequency for the oscillations seen in the experiment.

Our device [schematically shown in the inset of Fig. 1(a)] consists of a patterned high mobility GaAs/Al_xGa_{1-x}As heterostructure which contains a two-dimensional electron gas 65 nm below the surface. At $T=4.2$ K its electron density is $n_s=3\times 10^{15}$ m⁻² and the elastic mean free path is $l_e=8$ μm. The pattern was produced by electron beam lithography and transferred onto the sample by a carefully tuned wet etching step. The square geometry with a system dimension $L=2.4$ μm has quantum point contact (QPC)-like openings at its corners serving as contacts to the system. The openings are adjusted to support roughly three modes so that charging effects are not important. The whole structure is covered by a metal gate which allows one to tune the Fermi energy in the system. The sample is cooled in a dilution refrigerator with bath temperatures between 1.4 K and 30 mK. At low temperatures ($T<1$ K) both the elastic mean free path and the phase coherence length of the electrons exceed the dimensions of the device. Typical four-terminal measurements of the resistance $R_{ij,kl}=(V_k-V_l)/I$ are made by passing a current I through the contacts i and j and measuring the voltage drop across the other two contacts (k and l). The longitudinal resistance $R_L=R_{12,34}$ has a negative value at zero magnetic field; see Fig. 1(a). R_L then rises sharply and has a pronounced maximum at $B\approx 0.7B_c$ and a further one at $B\approx 2B_c$ (B_c is the magnetic field when the cyclotron radius at the Fermi energy, $R_c=\hbar k_F/eB$, equals side of the square, $2R_c=L$). The Hall resistance $R_H=R_{14,32}$ in this regime exceeds the linear value

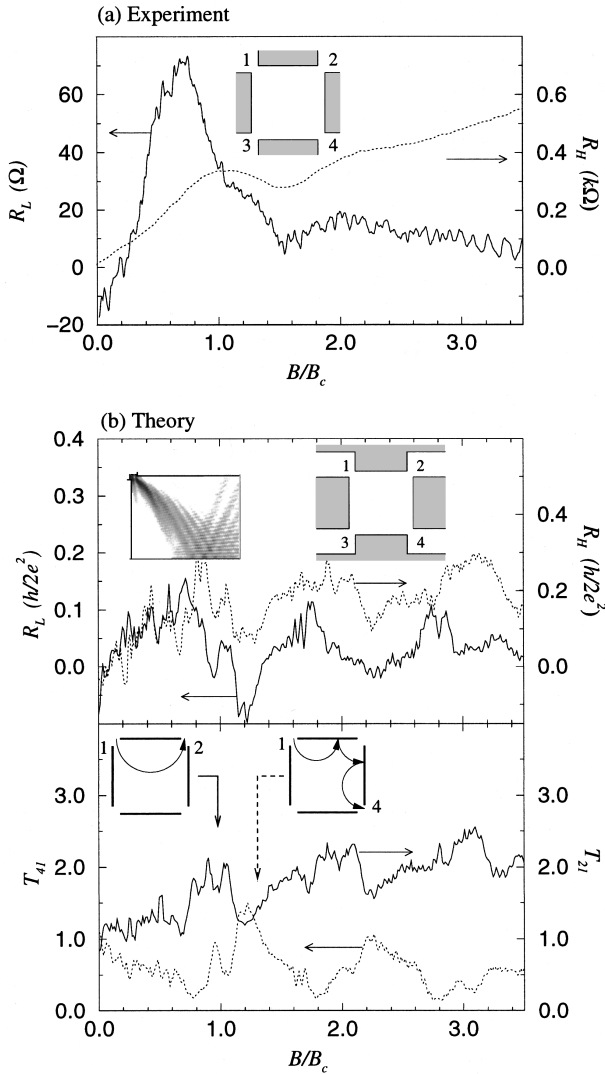


FIG. 1. (a) Measured longitudinal R_L and Hall resistance R_H for a ballistic square geometry (right inset); size of the square, $L=2.4 \mu\text{m}$, $T_{\text{bath}}=30 \text{ mK}$, B_c corresponds to the magnetic field when the cyclotron diameter equals to the size of the square, $B_c=75 \text{ mT}$. (b) Upper panel: calculated R_L and R_H in the four-terminal geometry shown in the inset; $L=1 \mu\text{m}$, $T=250 \text{ mK}$, $B_c=165 \text{ mT}$. Left inset shows collimated electron beam in a single QPC. Lower panel: transmission coefficients T_{21} and T_{41} ; the insets show classical ballistic trajectories illustrating the enhancement of T_{21} at $B \sim 0.9B_c$ and T_{41} at $B \sim 1.3B_c$ (peak positions differ from the classical expected values $B/B_c=1$ and 1.5 due to the strong collimation of the electron beam over the diagonal of the square).

$R_H=B/en_s$ and has plateaulike structures which are closely related to the corresponding features in R_L . For higher magnetic fields, $B \geq 0.2 \text{ T}$, Shubnikov–de Haas (SdH) oscillations and quantized Hall plateaus appear.

Figure 1(b) shows the results of numerical calculation for a square dot of size $L=1 \mu\text{m}$ in the four-terminal geometry depicted in the inset. R_L and R_H are computed in the framework of the multiterminal Landauer–Büttiker formalism.^{11–13} To calculate the transmission probabilities we solve a full quantum-mechanical scattering problem making use of the hybrid recursive Greens function technique,¹⁰ generalized for the presence of four leads. The effect of finite temperature is accounted for in a standard way, as a convolution of the transmission coefficients over energy, with the derivative of the Fermi-Dirac distribution.^{12,13}

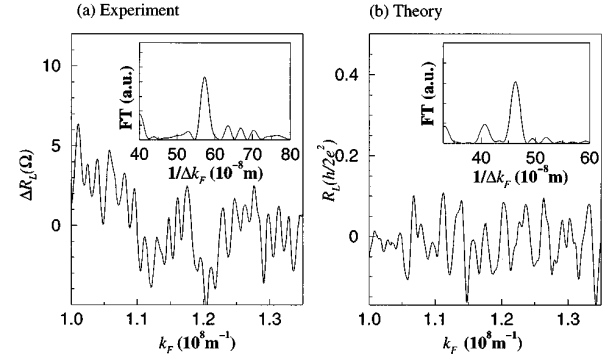


FIG. 2. Measured (a) and calculated (b) resistance oscillations as a function of the Fermi wave vector and their Fourier transforms (FT) (insets); $T_{\text{bath}}=30 \text{ mK}$ (a), $T=250 \text{ mK}$ (b). Periodicity of the measured and calculated oscillations as extracted from the FT, $\Delta k_F^{\text{exp}}=1.75 \times 10^6 \text{ m}^{-1}$, $\Delta k_F^{\text{num}}=2.17 \times 10^6 \text{ m}^{-1}$.

The dimension of the simulated device is smaller by a factor of 2.4 than the dimension of the real one (otherwise the calculation would become forbiddingly large). Therefore, one cannot expect a direct one-to-one correspondence between the experiment and the numerical simulations. At a given magnetic field the ratio R_c/L (and consequently, the spatial extent of the wave functions relative to the size of the square) is bigger for the simulated device. Therefore, interference effects are of a greater importance, giving rise to a rich structure which is not seen in the experiment. However, the relative peak positions of R_L, R_H are in good qualitative agreement. The lower panel of Fig. 1(b) shows the calculated total transmission coefficients, T_{21} and T_{41} , from lead 1 to leads 2 and 4, respectively (coefficients T_{31} and R_{11} are rather featureless and are not displayed here). Pronounced peaks seen in the transmission coefficients can be directly attributed to the classical ballistic orbits as depicted in the insets. An interplay between these coefficients in the four-terminal Landauer–Büttiker formula¹¹ causes the particular peak positions detected in both numerical simulations and experiment. A negative R_L seen in experimental and calculated longitudinal resistances at $B \sim 0$ is caused by the enhancement of the diagonal transmission ($T_{41} > T_{21}, T_{31}$) due to the classical horn collimation effect (see inset). Similar magnetoresistance anomalies related to the geometrical resonances and collimation effect have been detected in narrow junctions in Hall-bar geometry and are well explained within the classical ballistic transport picture (see Ref. 12 for a detailed review).

At lower temperatures ($T_{\text{bath}}=30 \text{ mK}$) reproducible ballistic fluctuations are superimposed on these classical effects in the experiment. This strongly suggests that these fluctuations are phase coherence effects arising from electron interference in the dot.

We tune the electron density, and thus the Fermi energy, inside the square by varying the voltage on the surface gate. At zero magnetic field we find a strong oscillatory behavior in both the experimental and the calculated longitudinal resistance as a function of $k_F=(2\pi n_s)^{1/2}$ (Fig. 2). In order to understand the nature of these periodic oscillations we study the probability density distribution $|\Psi(x,y)|^2$ in the dot. In this analysis we limit ourselves to a two-terminal geometry, where the dot is connected to reservoirs only by leads 1 and 2. (The calculated two-terminal resistance has the same fre-

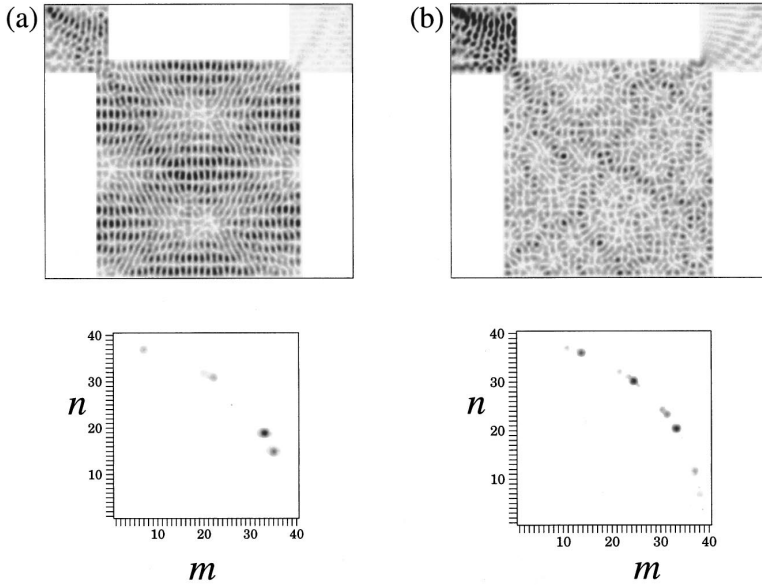


FIG. 3. Upper panel: probability density distribution $|\Psi(x,y)|^2$ in the dot calculated for $k_F = 1.12 \times 10^8 \text{ m}^{-1}$ (left) and $k_F = 1.134 \times 10^8 \text{ m}^{-1}$ (right). Lower panel: expansion coefficients $|c_{mn}|^2$ (see text) showing a contribution of the eigenstates m, n mediating transport at the given k_F .

quency of oscillations as the longitudinal four-terminal one and, therefore, the above limitation does not affect our conclusion on the origin of the fluctuations.)

In Fig. 3 $|\Psi(x,y)|^2$ is displayed for two representative values of k_F . The origin of the wave function pattern becomes clear when we numerically expand the calculated $\Psi(x,y)$ (which is a solution of the scattering problem in the open dot) onto the set of eigenstates of the square, $\psi_{mn} = (2/L)\sin(\pi mx/L)\sin(\pi ny/L)$ [with eigenenergies $\epsilon_{m,n} = \hbar^2/2m^*(k_m^2 + k_n^2)$; $k_m = \pi m/L$, $k_n = \pi n/L$]. This is equivalent to finding the coefficient c_{mn} of the complex two-dimensional sine-Fourier transform $\Psi(x,y) = \sum_m \sum_n c_{mn} \sin(\pi mx/L)\sin(\pi ny/L)$. The lower panel of Fig. 3 shows the calculated expansion coefficients $|c_{mn}|^2$ representing the contributions of the eigenstates m, n in the corresponding wave-function patterns. We find that only the coefficients c_{mn} with quantum numbers m, n lying near the circle of radius $R = \sqrt{m^2 + n^2} = k_F L / \pi$ give nonvanishing contributions. Broadening of the resonant levels due to the effect of the dot openings in k space is less than the distance between neighboring eigenstates whose quantum numbers differ by one, $|k_n - k_{n\pm 1}| = |k_m - k_{m\pm 1}| = \pi/L$. This makes us conclude that *transport in open structures is effectively mediated by the eigenstates of the corresponding closed dot with eigenenergies lying in close proximity to the Fermi energy, $\epsilon_{m,n} \approx E_F$* . By examining the wave function pattern as

k_F is varied, we are in a position to identify a particular set of eigenstates which contribute to the conductance at a given E_F . In the system under consideration where the aspect ratio “dot size/dot opening” is 10, the above set typically consists of just a few or sometimes even a single energy level.

At a given Fermi energy the eigenstates of the dot seem to be excited randomly at the circle $\sqrt{m^2 + n^2} = k_F L / \pi$, see Fig. 3, lower panel. However, averaging over the appropriate energy interval shows that it is primarily eigenstates with $m \approx n$ (i.e., $k_m \approx k_n \approx k_F / \sqrt{2}$), which mediate transport in the square dot, see Fig. 4(a). *It is the injection properties of the leads which define these selection rules*. Indeed, for a single QPC, a state with k_\perp inside the QPC is mostly coupled to an outgoing state with the same transverse wave vector.¹⁴ Although, strictly speaking, this is no longer correct for the double QPC’s in series (i.e., the dot) when interference effects destroy this coupling, it is justified when an average over a finite energy window is performed, so that the dot nominally plays the role of a reservoir.¹⁵ In the present geometry with electrons injected from a corner, the beam is strongly collimated due to a classical horn collimation effect and is directed along the diagonal of the box, Fig. 4(a). This means that $k_\perp \approx 0$ and $k_\parallel \approx k_F$. Extending those results for our geometry of the injecting leads, we get $\langle k_m \rangle \approx \langle k_n \rangle \approx k_F / \sqrt{2}$ which explains the above selection rules displayed in Fig. 4(a); ($\langle \dots \rangle$ stands for energy averaging). Note, that

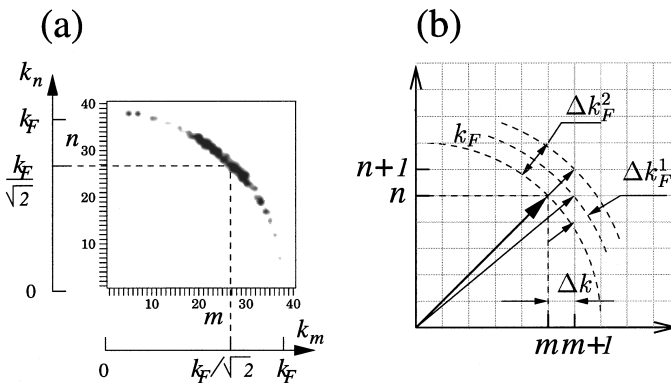


FIG. 4. (a) Coefficients $\langle c_{mn} \rangle$ averaged in the interval $1.1 < k_F < 1.15$ [20 patterns of $\Psi(x,y)$ have been analyzed]. (b) Eigenenergy states of the square dot which are excited as the Fermi energy is varied; see text.

the selection rule would be different for a different geometry of injecting leads.

Let us now discuss the observed periodicity of the conductance fluctuations. As we have found that the fluctuations are directly related to the excitation of resonant-energy levels of the dot, one can expect that the observed periodicity in k_F is related to the transitions between different eigenstates. Suppose, at a given k_F , that an eigenstate $\{m, n\}$ is excited in the dot; see Fig. 4(b). In the case under consideration mostly states with $k_m \approx k_n \approx k_F / \sqrt{2}$ are excited in the dot. For these states, changing k_F by $\Delta k_F^1 = \Delta k / \sqrt{2}$ results in the excitation of the states which one of the quantum number differs by unity, $\{m+1, n\}$ or $\{m, n+1\}$; $\Delta k = \pi/L$ being the distance between neighboring levels of the square. This, as one can expect, would lead to an appearance of the next conduction peak, with $\Delta k_F^1 L = \pi / \sqrt{2} = 2.22$ defining the period of the oscillations. Increasing k_F by $\Delta k_F^2 = 2\Delta k_F^1$ corresponds to the excitation of the state $\{m+1, n+1\}$ where both quantum numbers are changed by one. The calculated periodicity $\Delta k_F^{\text{num}} L = 2.22$, as extracted from the Fourier transform in Fig. 2, equals $\Delta k_F^1 L$ exactly. The observed periodicity, $\Delta k_F^{\text{exp}} L = 4.42$, however, rather well corresponds to $\Delta k_F^2 L = \sqrt{2}\pi = 4.44$.

Currently, we do not fully understand the origin of the factor of two disagreement between the theory and the experiment. We speculate, however, that this can be due to inelastic scattering which may play an important role in our relatively large dot, but has not been accounted for in the numerical simulations. Indeed, in the framework of the semiclassical theory,¹⁶ the contribution to the oscillating part of the density of states of the dot comes from the electrons bouncing in all stable primitive periodic orbits. In real system, however, phase breaking events and temperature smearing strongly suppress contributions from long orbits. In practice, neglecting periodic orbits or trajectories longer than the inelastic scattering length, l_i , seems to be a good approximation.^{4,17-19} The selection rules found above correspond to the excitation of the family of orbits with winding numbers (1,1) (Ref. 17) of length $l = 2\sqrt{2}L$, where the wave vectors (velocities) parallel to the sides of the square are equal, $k_m = k_n$. Note that in the dot under investigation, the lengths

of the longer primitive periodic orbits exceed l_i . When k_F is changed by Δk_F^1 , only k_m (or k_n) is changed and the final wave vectors are not equal. Then the electron no longer stays in the periodic orbit and eventually loses its phase memory after multiple bounces inside the dot, and does not contribute to phase-coherent interference. However, when k_F is changed by Δk_F^2 , both quantum numbers are changed such that $k_{m+1} = k_{n+1}$. As a result, the electron does not leave the periodic orbit and retains its phase coherence. We conclude this discussion with a question mark, in a hope that further experiments on much smaller dots, where electrons can perform tens or even hundreds of bounces before losing their phase coherence,²⁰ would help to clarify this issue.

Despite the discrepancy (factor of 2) between the experiment and the theory, it is still remarkable that they both demonstrate *periodic* conductance oscillations. This is in contrast to the *aperiodic* fluctuations seen in chaotic dots. The latter are well described by the random matrix theory,¹⁶ based on the assumption that the leads are coupled to a dot which is described by the transfer matrix constructed from the appropriate random statistical ensemble. In contrast, in the square dot only a set of selected eigenstates excited according to the specific selection rules effectively mediate transport through the structure. The fact that conductance oscillations in the dot are related to the excitation of the corresponding regular eigenstates of the square suggests that a soft potential due to remote donors would not affect the regular character of the electron dynamics significantly.

To conclude, at low magnetic fields the magnetoresistance is dominated by phenomena that depend on classical trajectories traversing a ballistic square cavity. Conductance fluctuations observed at millikelvin temperature are directly related to the excitation of a particular set of eigenstates of the square selected according to injection properties of leads. The above selection rule sets a specific frequency for the oscillations seen in the experiment.

We thank J. P. Kotthaus, S. Ulloa, Y. Levinson and J. P. Bird for valuable discussions. This work was partly supported by a grant from Deutsche Forschungsgemeinschaft (SFB 348) (R.S.). I.V.Z. acknowledges a grant from the Royal Swedish Academy of Sciences.

¹R. Blümel and U. Smilansky, Phys. Rev. Lett. **60**, 477 (1988); R. A. Jalabert *et al.*, *ibid.* **65**, 2442 (1990); H. U. Baranger *et al.*, *ibid.* **70**, 3876 (1993); H. U. Baranger and P. A. Mello, *ibid.* **73**, 142 (1994); R. A. Jalabert *et al.* Europhys. Lett. **27**, 255 (1994).
²M. J. Berry *et al.*, Surf. Sci. **305**, 495 (1994); H. Chan *et al.*, Phys. Rev. Lett. **74**, 3876 (1995); M. Persson *et al.*, Phys. Rev. B **52**, 8921 (1995); J. P. Bird *et al.*, *ibid.* **52**, 8295 (1995); M. W. Keller *et al.*, *ibid.* **53**, R1693 (1996); J. P. Bird *et al.*, Europhys. Lett. **35**, 529 (1996).
³A. M. Chang *et al.*, Phys. Rev. Lett. **73**, 2111 (1994); C. Marcus *et al.*, CHAOS **3**, 634 (1993); J. P. Bird *et al.*, Phys. Rev. B **52**, 14 336 (1995).
⁴S. M. Reiman *et al.*, Z. Phys. B **101**, 377 (1996).
⁵K.-F. Berggren *et al.*, Phys. Rev. B **54**, 11 612 (1996).
⁶Y. Wang *et al.*, Phys. Rev. B **53**, 16 408 (1996).
⁷H. Ishio, J. Stat. Phys. **83**, 203 (1995).
⁸P. Šeba, Phys. Rev. B **53**, 13 024 (1996).
⁹K.-F. Berggren and Z.-L. Ji, CHAOS **6**, 543 (1996).

¹⁰I. V. Zozoulenko *et al.*, Phys. Rev. B **53**, 7975 (1996); **53**, 7987 (1996).
¹¹M. Büttiker, Phys. Rev. Lett. **57**, 1761 (1986).
¹²C. W. J. Beenakker and H. van Houten, *Solid State Physics, Advances in Research and Applications* (Academic, San Diego, 1991), Vol. 44.
¹³S. Datta, *Electronic Transport in Mesoscopic Systems* (Cambridge University Press, Cambridge, England, 1995).
¹⁴A. Szafer and A. D. Stone, Phys. Rev. Lett. **62**, 300 (1989).
¹⁵I. V. Zozoulenko and K.-F. Berggren, Phys. Rev. B **54**, 5823 (1996).
¹⁶M. C. Gutzwiller, *Chaos in Classical and Quantum Mechanics* (Springer-Verlag, New York, 1991).
¹⁷F. von Oppen, Phys. Rev. B **50**, 17 151 (1994).
¹⁸K. Richter *et al.*, Phys. Rev. B **54**, R5219 (1996).
¹⁹C. D. Schwieters *et al.*, Phys. Rev. B **54**, 10 652 (1996).
²⁰J. B. Bird *et al.*, Phys. Rev. B **51**, 18 037 (1995); R. M. Clarke *et al.*, *ibid.* **52**, 2656 (1995).